



HAL
open science

Metamorphic high electron mobility Te-doped AlInSb/GaInSb heterostructures on InP (001)

G. Delhaye, L. Desplanque, X. Wallart

► **To cite this version:**

G. Delhaye, L. Desplanque, X. Wallart. Metamorphic high electron mobility Te-doped AlInSb/GaInSb heterostructures on InP (001). *Journal of Applied Physics*, 2008, 104 (6), pp.066105. 10.1063/1.2978365 . hal-00356944

HAL Id: hal-00356944

<https://hal.science/hal-00356944>

Submitted on 25 May 2022

HAL is a multi-disciplinary open access archive for the deposit and dissemination of scientific research documents, whether they are published or not. The documents may come from teaching and research institutions in France or abroad, or from public or private research centers.

L'archive ouverte pluridisciplinaire **HAL**, est destinée au dépôt et à la diffusion de documents scientifiques de niveau recherche, publiés ou non, émanant des établissements d'enseignement et de recherche français ou étrangers, des laboratoires publics ou privés.

Metamorphic high electron mobility Te-doped AlInSb/GaInSb heterostructures on InP (001)

Cite as: J. Appl. Phys. **104**, 066105 (2008); <https://doi.org/10.1063/1.2978365>

Submitted: 16 May 2008 • Accepted: 18 July 2008 • Published Online: 18 September 2008

G. Delhaye, L. Desplanque and X. Wallart



View Online



Export Citation

ARTICLES YOU MAY BE INTERESTED IN

Molecular beam epitaxial growth of metamorphic AlInSb/GaInSb high-electron-mobility-transistor structures on GaAs substrates for low power and high frequency applications

Journal of Applied Physics **109**, 033706 (2011); <https://doi.org/10.1063/1.3544041>

Band parameters for III-V compound semiconductors and their alloys

Journal of Applied Physics **89**, 5815 (2001); <https://doi.org/10.1063/1.1368156>

Dislocation filtering by $\text{Al}_x\text{In}_{1-x}\text{Sb}$ / $\text{Al}_y\text{In}_{1-y}\text{Sb}$ interfaces for InSb-based devices grown on GaAs (001) substrates

Applied Physics Letters **88**, 191908 (2006); <https://doi.org/10.1063/1.2203223>

Lock-in Amplifiers
up to 600 MHz



Zurich
Instruments



Metamorphic high electron mobility Te-doped AlInSb/GaInSb heterostructures on InP (001)

G. Delhaye,^{a)} L. Desplanque, and X. Wallart^{b)}

Institut d'Electronique de Microelectronique et de Nanotechnologie, UMR CNRS 8520, Avenue Poincaré, B.P. 60069, 59652 Villeneuve d'Ascq, France

(Received 16 May 2008; accepted 18 July 2008; published online 18 September 2008)

This work reports on the Te δ -doping of high electron mobility AlInSb/GaInSb heterostructures grown by molecular beam epitaxy on InP(001) substrates with a metamorphic approach. The combination of atomic force microscopy and van der Pauw measurements is used to investigate and explain the influence of the buffer layers on the electron mobility and sheet density in the heterostructure. Furthermore, a significant increase in the electron sheet density is reached when the δ -doping plane is incorporated in a thin AlSb layer introduced in the barrier. This improvement is explained by the lower dopant activation energy in the AlSb layer. AlInSb/GaInSb heterostructures with an electron mobility of 18 000 cm²/V s and sheet density of 2.2×10^{12} cm⁻² at room temperature are demonstrated. © 2008 American Institute of Physics. [DOI: 10.1063/1.2978365]

With their electronic properties, antimony-based compounds are of great interest in the elaboration of innovative components.¹ Heterostructures with original band offsets could be obtained in electronic devices such as resonant tunneling diode² or heterojunction bipolar transistor.³ Furthermore, their low effective mass and small band gap make antimonides promising materials for ultrahigh speed field effect transistors and low power consumption devices, such as high electron mobility transistor.^{4,5} Two good candidates to reach very high electron mobility heterostructures are AlSb/InAs and AlInSb/InSb systems. Kroemer was the pioneers in the development of the former on GaAs(001). Electron mobilities higher than 30 000 cm²/V s combined with sheet electron densities of 1.5×10^{12} cm⁻² were obtained at room temperature.⁵ Nevertheless, the associated transistor performances are limited by a large charging effect of the substrate and parasitic gate leakage current due to the type II configuration of the AlSb/InAs heterostructure. The AlInSb/InSb system was recently demonstrated by Ashley *et al.*⁶ They measured an electron mobility of about 17 000 cm²/V s with a carrier density of 2×10^{12} cm⁻² at room temperature in a strained InSb quantum well confined between Al_{0.15}In_{0.85}Sb barriers. However, the electron sheet density in the channel is limited since the conduction band (CB) offset is only about 150 meV. The Al_{0.55}In_{0.45}Sb/Ga_{0.5}In_{0.5}Sb system may be a valuable trade-off. Indeed, it is a type I heterostructure with an expected electron effective mass in the channel close to the InAs one (0.025 m_0) and a CB offset near 0.5 eV. Furthermore, with its high hole mobility,⁷ GaInSb can be a good option for complementary circuits in advanced logic applications.

In the present work, we report on Te δ -doped AlInSb/GaInSb heterostructures. We show the influence of the growth parameters, mainly the buffer layer and the material

fitting the Te δ -doping plane, on the transport properties of the heterostructure.

The heterostructures were grown on a 3 in. RIBER Compact 21TM molecular beam epitaxy reactor with a base pressure better than 1×10^{-10} Torr. Group III materials and tellurium were deposited by thermal evaporation from effusion cells. GaTe was used as *n*-type dopant source and valve cracker cells were used to produce As₂ and Sb₂. The fluxes were calibrated using reflection high energy electron diffraction (RHEED) specular beam intensity oscillations on GaAs, GaSb, and InAs substrates. For all samples, a V/III ratio between 2 and 3 was used. The samples have been characterized by atomic force microscopy (AFM) using a Digital Nanoscope III instrument working in the tapping mode and by Hall effect using Van Der Pauw measurements.

As no semi-insulating lattice matched substrate exists, a metamorphic approach is required for the growth of the Al_{0.55}In_{0.45}Sb/Ga_{0.5}In_{0.5}Sb heterostructure. InP(001) semi-insulating substrate was chosen for its closest lattice parameter. The misfit between the two compounds is equal to 7.15%. Three different metamorphic buffers have been compared to obtain the best mobility (Fig. 1). The first one (buffer 1) consists of a 1.4- μ m-thick Al_{0.55}In_{0.45}Sb grown directly at 480 °C on a 100 nm AlInAs layer lattice matched

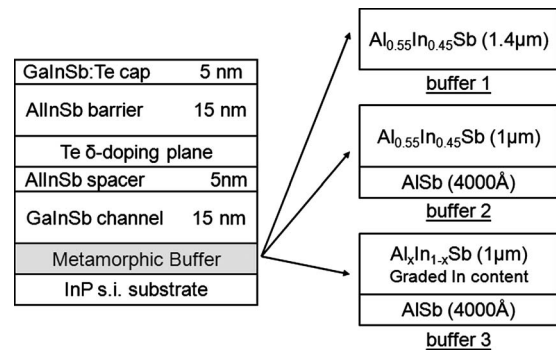


FIG. 1. Te δ -doped heterostructure with the three buffers studied in the present work.

^{a)}Electronic mail: gabriel.delhaye@iemn.univ-lille1.fr.

^{b)}Electronic mail: xavier.wallart@iemn.univ-lille1.fr.

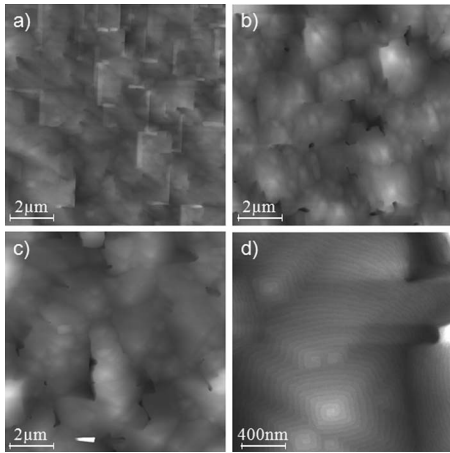


FIG. 2. $10 \times 10 \mu\text{m}^2$ AFM images on top of (a) buffer 1, (b) buffer 2, and (c) buffer 3; (d) AFM image on top of buffer 3. For the images (a)–(c), the Z-scale varies from 0 to 30 nm. For the last image, the scale varies from 0 to 8 nm.

to InP. In this case, the RHEED pattern exhibits a three-dimensional (3D) growth mode at the beginning of the $\text{Al}_{0.55}\text{In}_{0.45}\text{Sb}$ growth and then turns to a two-dimensional growth mode. For the second design (buffer 2), a two step buffer is used with a 400 nm AISb layer grown at 510°C inserted between AlInAs and a $1\text{-}\mu\text{m}$ -thick $\text{Al}_{0.55}\text{In}_{0.45}\text{Sb}$ layer grown at 480°C . The AISb deposition on AlInAs turns rapidly into a 3D surface that is smoothed during the subsequent AISb growth. The transition from AISb to $\text{Al}_{0.55}\text{In}_{0.45}\text{Sb}$ is characterized by a slight surface roughening. For the last buffer (buffer 3), the $1\text{-}\mu\text{m}$ -thick $\text{Al}_{0.55}\text{In}_{0.45}\text{Sb}$ layer is replaced by a graded $\text{Al}_{1-x}\text{In}_x\text{Sb}$ one with x linearly increased from 10% to 50% on a 800 nm thickness and then step decreased to 45% for a 200 nm final uniform part. The active part of the heterostructure (referenced as structure A) is grown at 450°C and consists of a 15 nm $\text{Ga}_{0.5}\text{In}_{0.5}\text{Sb}$ channel, a 5 nm $\text{Al}_{0.55}\text{In}_{0.45}\text{Sb}$ spacer, a Te δ -doping plane, a 150 nm $\text{Al}_{0.55}\text{In}_{0.45}\text{Sb}$ barrier, and a 5 nm $\text{Ga}_{0.5}\text{In}_{0.5}\text{Sb}$ Te-doped cap layer (Fig. 1). The growth of the channel started at 450°C and is further decreased to 410°C in the Te δ -doping plane to avoid tellurium segregation.

The samples have been first characterized by double x-ray diffraction using the (004) reflection. No significant difference between the three buffers could be observed as regards the strain relaxation of the $\text{Al}_{0.55}\text{In}_{0.45}\text{Sb}$ layer. On the contrary, the 300 K electron mobilities are 10 000, 13 000, and 18 000 $\text{cm}^2/\text{V}\cdot\text{s}$ for buffers 1, 2, and 3, respectively. AFM images of the buffer surfaces are presented in Figs. 2(a)–2(c). All samples exhibit a surface morphology composed of pyramidal mounds, associated with a spiral growth due to the presence of threading dislocations.⁸ In spite of rather similar rms roughness values (~ 3 nm), the mean separation distance between the mounds, i.e., the roughness length scale, increases from $0.8 \mu\text{m}$ for buffer 1 to $3 \mu\text{m}$ for buffer 3. This latter presents the most ordered surface and it probably explains why the related heterostructure exhibits the highest mobility. Consequently, we use buffer 3 for the growth of the following structures.

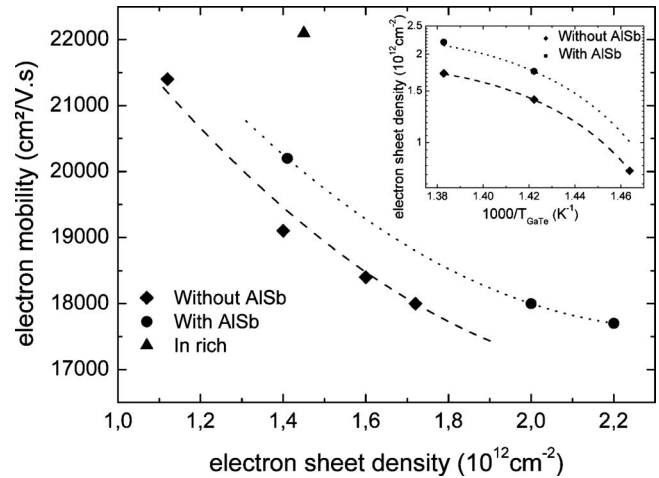


FIG. 3. Electron mobility vs the electron sheet density in different heterostructures. In the inset, the electron sheet density vs the GaTe source temperature is represented. Dashed and dotted lines are only guides for eyes.

In Fig. 3, diamonds present the electron mobility measured for different electron sheet densities in the channel. These values were obtained by varying the Te density in the doping plane. We observe a characteristic decrease in electron mobility when the sheet carrier density is increased. However, a doping efficiency higher than $1.7 \times 10^{12}/\text{cm}^2$ is difficult to achieve as can be seen in the inset of Fig. 3 describing the evolution of sheet carrier density versus the inverse of the GaTe effusion cell temperature.

Hill *et al.*⁹ studied the influence of DX-centers in Te-doped AlInSb in function of the alloy composition. They measured a strong dependence of the donor activation energy on the indium content. The maximum value (125 meV) is reached for an alloy composition close to the direct-indirect crossover point (around 30% of indium). This activation energy is still high for an indium fraction of 45% (~ 70 meV) whereas it is lower for AISb (40 meV). A high activation energy of Te in the doping plane leads to a lower effective CB offset at the InAISb/InGaSb heterojunction and results in a poor transfer efficiency and a low sheet carrier density.

To overcome this limitation, we studied two other structures using the buffer 3. In the first one (referenced as structure B), three AISb monolayers were added before and after the Te δ -doping. In the second one (structure C), the indium content was increased to 65% and 60% in the channel and the barrier layer, respectively. Circles in the inset of Fig. 3 present the sheet carrier density obtained with structure B. We observe an increase of 30% of the doping efficiency when Te is incorporated in AISb. For the structure C, a 15% lower doping efficiency is obtained. The former result agrees with the observations of Hill *et al.* Indeed, the insertion of the doping plane in AISb leads to a lower activation energy of Te dopants and to a higher effective CB offset at the heterojunction. Furthermore, as can be seen in Fig. 3 (circles), the electron mobility is not affected. However, contrary to what could be expected from Hill *et al.* results, the In-content increase does not lead to a higher electron sheet density. This is probably due to a reduction in the CB offset for high indium contents. Nevertheless, thanks to the lower

TABLE I. Electron sheet density and mobility at $T=300$ and 77 K with $T_{\text{GaTe}}=450$ °C.

Structure sample	Electron mobility ($\text{cm}^2/\text{V s}$)		Electron sheet density (cm^{-2})	
	$T=300$ K	$T=77$ K	$T=300$ K	$T=77$ K
A	18 800	...	1.7×10^{12}	...
B	17 700	34 700	2.2×10^{12}	2.2×10^{12}
C	22 100	44 900	1.4×10^{12}	1.3×10^{12}

electron effective mass in the channel, a larger electron mobility ($22\,100\text{ cm}^2/\text{V s}$ at 300 K , triangle in Fig. 3) is reached.

Table I gathers the best results we have obtained. They are comparable with those obtained within the $\text{Al}_{0.15}\text{In}_{0.85}\text{Sb}/\text{InSb}$ system by Ashley *et al.*⁶ for the same sheet carrier density although the electron effective mass in the channel material used here ($\text{Ga}_{0.5}\text{In}_{0.5}\text{Sb}$) is heavier than in InSb. Nevertheless, the electron mobility remains lower than in the AlSb/InAs system, for which values of $23\,000$ and $65\,900\text{ cm}^2/\text{V s}$ at 300 and 77 K , respectively, were demonstrated¹⁰ for a sheet carrier density around $2.1 \times 10^{12}\text{ cm}^{-2}$. The main reason for this mobility limitation is the high threading dislocation density. Even in the best case [buffer 3, Figs. 2(c) and 2(d)] the density of threading dislocations estimated from the AFM images remains in the $10^8\text{--}10^9/\text{cm}^2$ range. It appeals for a further optimization of the buffer layer via “an interface misfit array,”¹¹ to allow both for strain relaxation and a low threading dislocation density.

This work demonstrates high electron mobility Te δ -doped AlInSb/GaInSb heterostructures. The best results are obtained for a buffer comprising a uniform AlSb layer and a

linear graded $\text{Al}_x\text{In}_{1-x}\text{Sb}$ one. The addition of a thin AlSb layer below and beyond the doping plane increases the yield of the electronic transfer into the channel without electron mobility degradation. The electron sheet density gain seems to be related to the different donor activation energies in AlSb and $\text{Al}_{0.55}\text{In}_{0.45}\text{Sb}$. Our preliminary electron sheet density and mobility values at room temperature are promising and comparable with those of the $\text{Al}_{0.15}\text{In}_{0.85}\text{Sb}/\text{InSb}$ heterostructures.

We would like to thank J.-L. Codron for his help in preparation and growth of the samples. This work has been achieved with the financial support of the European Union, the French Government, and the Regional Council.

¹B. R. Bennett, R. Magno, J. B. Boos, W. Kruppa, and M. G. Ancona, *Solid-State Electron.* **49**, 1875 (2005).

²L. F. Luo, R. Beresford, and W. I. Wang, *Appl. Phys. Lett.* **53**, 2320 (1988).

³R. Magno, J. B. Boos, P. M. Campbell, B. R. Bennett, E. R. Glaser, B. P. Tinkham, M. G. Ancona, K. D. Hobart, D. Park, and N. A. Papanicolaou, *Electron. Lett.* **41**, 370 (2005).

⁴G. Tuttle, H. Kroemer, and J. H. English, *J. Appl. Phys.* **65**, 5239 (1989).

⁵H. Kroemer, *Physica E (Amsterdam)* **20**, 196 (2004).

⁶T. Ashley, L. Buckle, S. Datta, M. T. Emeny, D. G. Hayes, K. P. Hilton, R. Jefferies, T. Martin, T. J. Phillips, D. J. Wallis, P. J. Wilding, and R. Chau, *Electron. Lett.* **43**, 777 (2007).

⁷B. R. Bennett, M. G. Ancona, J. B. Boos, and B. V. Shanabrook, *Appl. Phys. Lett.* **91**, 042104 (2007).

⁸P. M. Thibado, B. R. Bennett, M. E. Twigg, B. V. Shanabrook, and L. J. Whitman, *J. Vac. Sci. Technol. A* **14**, 885 (1996).

⁹P. Hill, N. Weisse-Bernstein, L. R. Dawson, P. Dowd, and S. Krishna, *Appl. Phys. Lett.* **87**, 092105 (2005).

¹⁰L. Desplanque, D. Vignaud, and X. Wallart, *J. Cryst. Growth* **301–302**, 194 (2007).

¹¹S. H. Huang, G. Balakrishnan, A. Khoshakhlagh, A. Jallipalli, L. R. Dawson, and D. L. Huffaker, *Appl. Phys. Lett.* **88**, 131911 (2006).